



Article

Characterization and Biological Studies of Synthesized Titanium Dioxide Nanoparticles from Leaf Extract of *Juniperus phoenicea* (L.) Growing in Taif Region, Saudi Arabia

Luluah M. Al Masoudi ¹, Abeer S. Alqurashi ¹, Abeer Abu Zaid ²  and Hamida Hamdi ^{1,*} ¹ Department of Biology, College of Science, Taif University, P.O. Box 11099, Taif 21944, Saudi Arabia² Department of Food Science and Nutrition, Alkhurmah University College, Taif University, P.O. Box 11099, Taif 21974, Saudi Arabia

* Correspondence: shimaa76sl@tu.edu.sa

Abstract: Green synthesis of metal nanoparticles in nanosized form has acquired great interest in the area of nanomedicine as an environmentally friendly and cost-effective alternative compared to other chemical and physical methods. This study deals with the eco-friendly green synthesis of titanium dioxide nanoparticles (TiO₂ NPs) utilizing *Juniperus phoenicea* leaf extract and their characterization. The biosynthesis of TiO₂ NPs was completed in 3 h and confirmed by UV-Vis spectroscopy, a strong band at 205.4 nm distinctly revealed the formation of NPs. Transmission electron microscopy (TEM) analysis showed the synthesized TiO₂ NPs are spherical in shape, with a diameter in a range of 10–30 nm. The XRD major peak at 27.1° congruent with the (110) lattice plane of tetragonal rutile TiO₂ phase. Dynamic light scattering (DLS) analysis revealed synthesized TiO₂ NPs average particle size (hydrodynamic diameter) of (74.8 ± 0.649) nm. Fourier transmission infrared (FTIR) revealed the bioactive components present in the leaf extract, which act as reducing and capping agents. The antimicrobial efficacy of synthesized TiO₂NPs against, *Staphylococcus aureus*, and *Bacillus subtilis* (Gram-positive), *Escherichia coli* and *Klebsiella pneumoniae* (Gram-negative), Yeast strain (*Saccharomyces cerevisiae*) and fungi (*Aspergillus niger*, and *Penicillium digitatum*) assayed by a disc diffusion method. TiO₂NPs inhibited all tested strains by mean inhibition zone (MIZ), which ranged from the lowest 15.7 ± 0.45 mm against *K. pneumoniae* to the highest 30.3 ± 0.25 against *Aspergillus niger*. The lowest minimum inhibitory concentration (MIC) and bactericidal (MBC) values were 20 µL/mL and 40 µL/mL of TiO₂NPs were observed against *Asp. niger*. Moreover, it showed significant inhibitory activity against human ovarian adenocarcinoma cells with IC₅₀ = 50.13 ± 1.65 µg/mL. The findings concluded that biosynthesized TiO₂ NPs using *Juniperus phoenicea* leaf extract can be used in medicine as curative agents according to their in vitro antibacterial, antifungal, and cytotoxic activities.

Keywords: Titanium dioxide nanoparticles; *Juniperus phoenicea*; green synthesis; antimicrobial potential; anticancer effect



Citation: Al Masoudi, L.M.; Alqurashi, A.S.; Abu Zaid, A.; Hamdi, H. Characterization and Biological Studies of Synthesized Titanium Dioxide Nanoparticles from Leaf Extract of *Juniperus phoenicea* (L.) Growing in Taif Region, Saudi Arabia. *Processes* **2023**, *11*, 272. <https://doi.org/10.3390/pr11010272>

Academic Editors: Ticuta Negreanu-Pirjol, Ana Maria Stanciu, Bogdan-Stefan Negreanu-Pirjol and Clara Grosso

Received: 23 November 2022

Revised: 9 January 2023

Accepted: 11 January 2023

Published: 14 January 2023



Copyright: © 2023 by the authors. Licensee MDPI, Basel, Switzerland. This article is an open access article distributed under the terms and conditions of the Creative Commons Attribution (CC BY) license (<https://creativecommons.org/licenses/by/4.0/>).

1. Introduction

The genus *Juniperus* is considered a major member of Cupressaceae family. About fifty and sixty-seven species of juniper are vastly scattered around worldwide, the Northern Hemisphere, from the Arctic, south to tropical Africa in the Old World, and to the mountains of Central America. Juniper has needle-like leaves, and its fruits are called berries. *Juniperus communis* Berries are used as a spice, in European cuisine [1] as a female contraceptive, and to treat diabetes by Native Americans [2]. The berries of *Juniperus phoenicea* were found in ancient Egyptian tombs [3] growing in Egypt in Sinai and, the Mediterranean region [4]. Phytochemical examination of the leaves and fruits of the plant showed that they are rich in essential oil, carbohydrates, and/or glycosides, sterols and/or triterpenes, and flavonoids [5]. All alcoholic extracts of the aerial parts of *Juniperus phoenicea* collected from Libya showed high significant cytotoxic activity against breast and colon cell lines MCF-7

and HCT-116, as well as antibacterial activity against Gram-positive and Gram-negative bacteria [6]. Several authors have investigated the effect of the berries of juniper as a potential remediation for diet-controlled diabetes [7]. The leaf powder is taken as a remedy for bronchi diseases or as a diuretic. Tar of this species is used as an alternative to Barbary rice, as an intestinal remedy for Children [8], and dried fruits Powder can be used to heal skin ulcers and abscesses. The mixture of leaves and fruits is used as an oral hypoglycemic agent [9]. Juniper wood is used in the carpentry in Algeria and Tunisia; moreover, it is mainly used for charcoal and fuel production in Africa [10,11]. The medicinal utilizations of *Juniperus* plants are spread in Saudi Arabia, Lebanon, Bosnia, and Turkey and according to folk medicine; it has been used to treat the diseases of respiratory tract and skin [12], rheumatism, gall bladder stones, and urinary problems [13].

Green preparation is a substitutional route for approaching nanoparticles (NPs) utilizing natural resources such as medicinal plants and microorganisms as reducing agents. Being low cost-effective, biocompatible, stable, environmental friendly, less toxic and secure for diagnostic and curative purposes, green synthesis is an emerging way for the synthesis of NPs of various materials [14–17]. Several studies successfully synthesized TiO_2 utilizing various plant extracts [18–20]. Presence of phytochemicals is the main mechanism considered for plant-mediated nanoparticle synthesis. The reduced ions from different materials such as terpenoids, flavonoids, quinones, carboxylic acids, ketones, aldehydes, and amides are the main causes of the mandatory responsibility of phytochemicals. In this area, many works are provided by biosynthesizing routes of plants and plant leaf extract [21,22]. In this area, *Juniperus phoenicea* leaf extract will be a possible candidate for the preparation of NPs according to their different phytoconstituents [5].

Several studies on the antimicrobial efficacy of NPs such as Al, Ag, Au, CuO, MgO, TiO_2 etc., are effective against many drug-resistant strains of bacteria, fungi, and viruses [23]. Therefore, NPs have the potency to act as a substitute to antibiotics and to control microbial infections caused by *Staphylococcus epidermidis*, *Staphylococcus aureus*, *Salmonella typhi*, and *Klebsiella pneumoniae* [24]. Among the metal oxide NPs, TiO_2 nanoparticles are the most outstanding nanomaterial due to their chemical stability, photocatalytic characteristics, and non-toxicity. They have been tremendously used in many fields such as cosmetics industry, electrochemical devices, solar cells; antibacterial coatings and pollution management [25]. Wild medicinal plants are rich in flavonoids that have been identified as beneficial components in the treatment of cancer. Green synthesis of NPs using natural sources such as extracts of wild medicinal plants is a novel approach resulting in an anticancer effect. Nanomedicine is the usage of nanotechnology in the examination, diagnosis, and treatment, of many diseases, including cancer [26–29]. It provides complete steps and estimations against cancer through cancer foretelling and diagnostics, treatment and protection, as well as potential individualized remediation [26–28].

To the best of available knowledge, there is still no report on the TiO_2 nanoparticles synthesis using *Juniperus phoenicea* leaf extract. The biosynthesized TiO_2 nanoparticles were characterized by ultraviolet-visible spectroscopy (UV-Vis), dynamic light scattering (DLS), transmission electron microscopy (TEM), X-ray diffraction (XRD), Fourier transmission infrared (FTIR), techniques. Furthermore, the goal is to estimate the antimicrobial and anticancer efficacy of biosynthesized TiO_2 NPs which are not yet reported.

2. Materials and Methods

2.1. Collection of Plant Samples

The plant samples of *Juniperus phoenicea* were gathered from different areas of Taif, Saudi Arabia, and taxonomically identified. The plant samples were dried in air and then ground to a fine powder.

2.2. Extraction of Green Plants

Extraction of green plant powder as well as the bio-synthesis of TiO_2 NPs was achieved according to [30] with some modifications. Fresh plant powder (10 g) was boiled in 60%

ethanol (100 mL) for 2 min and soaked overnight in the same solution at 60 °C. Through Whatman filter paper No.1, the mixture was filtered thrice and diluted with distilled deionized water in a ratio of 1:4.

2.3. GC/MS Analysis of *Juniperus phoenicea* Leaf Aqueous Extract

GC/MS analysis was carried out in a coupled 7890A gas chromatograph system (Agilent 19091-433HP, Agilent Technologies, Santa Clara, CA, USA) with a HP-5 MS fused silica column (30.0 m × 250 µm × 0.25 µm). The oven temperature was set initially at 50 °C for 1 min and temperature was increased at a rate of 10 °C min⁻¹ till 125 °C and it was further increased till 5270 °C (5 min) at a rate of 5 °C min⁻¹. Sample injection temperature was set at 250 °C. About 100 µL sample was injected with helium gas as carrier (flow rate of 1.0 mL min⁻¹). The percentage composition was determined by comparing the peak area to total area. The content analysis was carried out by MS solution software and also comparing the National Institute of Standards and Technology (NIST) database [31].

The GC-MS method was used to analyze the predominant phytochemicals present in the *J. phoenicea* leaf aqueous extract; where the gas chromatography separates the individual compounds in the extract, whereas the MS helps to predict the possible compounds based on the m/z values obtained.

2.4. Bio-Synthesis and Purification of TiO₂ NPs

The TiO₂ NPs synthesis was performed by incubating 100 mL of plant extracts with 900 mL of the freshly prepared aqueous solution of 25 mM Titanium dioxide (TiO₂) at 60 °C. The TiO₂ NPs were attained by incubating the reaction mixture at 60 °C for 2 h or until the formation of a white precipitate of TiO₂ NPs.

The resulting TiO₂ NPs were purified by centrifugation at 13,000 rpm for 20 min, then washed the pellets containing nanoparticles thrice with distilled deionized water and then air-dried.

2.5. Characterization of TiO₂ Nanoparticles

2.5.1. UV-Visible Spectra Analysis

The optical properties of the prepared TiO₂ NPs were analyzed by using UV-visible spectrophotometer (Shimadzu, Kyoto, Japan). Briefly, the sample (3 mL) was taken in a quartz cuvette and further scanned in the wavelength range of 200–800 nm (resolution of 1 nm). The resulting spectrum was collected using the spectrophotometer software and major peaks were identified [32].

The UV/visible spectrophotometry provides reliable data on the absorption maxima of the test sample and thereby helps to corroborate it with the absorption maxima of the major compounds identified in GC-MS analysis.

2.5.2. Dynamic Light Scattering (DLS)

The spectroscatterer RiNA, GmbH class3B was used to determine DLS measurements (the main size and distribution size) of the TiO₂ NPs. The dried powder was scattered in distilled water and all analyses were performed at 20 °C for ten cycles. The experiments for DLS were repeated three times.

The non-destructive morphological analysis technique of dynamic light scattering had been applied in phytocomponent analysis. It is highly useful for the accurate sizing of chemical and physical materials that are synthesized using plant phytochemicals.

2.5.3. Transmission Electron Microscopy (TEM)

JEOL model JEM-2000FX instrument operated at an accelerating voltage of 200 Kilo voltage used to determine TEM measurement (particle size and morphology of the surface) of the synthesized nanoparticles. A few drops of sonicated powdered sample were prepared and placed on a carbon-coated copper grid and dried in air for 1 h. Finally, the

energy dispersive X-ray (EDX, Model EVO-40, ZEISS) spectrum for elemental analysis was recorded.

2.5.4. X-ray Diffraction Spectroscopic Analysis (XRD)

XRD technique is used to study the crystalline or amorphous nature and the structure of the synthesized TiO₂ NPs. Then the powdered sample was placed on a Shimadzu XRD-6000 and set in the range of 5–50° at a 2θ angle [32].

2.5.5. Fourier Transform Infrared Spectroscopy (FTIR)

Initially, the potassium bromide (KBr) pellet (FTIR grade) method in 1:100 was used for FTIR analysis of the dried TiO₂ NPs to identify the functional group, which is responsible for the formation of TiO₂ NPs synthesized by *Juniperus phoenicea* leaf extract. The spectrum of the sample by Jasco FT/IR-6300 FTIR-spectrometer with wave number in the range of 400 cm^{−1} to 4000 cm^{−1} [33,34].

FTIR is highly useful to identify the class of compounds by analyzing the respective spectral maxima. Every class of compounds, under their bonding and functional group present, expresses some major IR absorbance maxima. This tool is helpful to confirm the class of compounds and their important functional groups such as polyphenols, carbonyls, hydroxyl, and alkenes.

2.6. Antimicrobial Efficacy of TiO₂ NPs

Disc diffusion assay was used to determine the antimicrobial efficacy of TiO₂ NPs against the tested strains. This method was previously explained by [35]. A list of microbial strains namely *E. coli* and *Klebsiella pneumoniae* as Gram-negative bacteria, *S. aureus* and *Bacillus cereus* as Gram-positive bacteria, yeast strain (*Saccharomyces cerevisiae*), and fungal strains (*Aspergillus niger*, *Penicillium digitatum*) were used. Bacterial and fungal strains used for the antimicrobial evaluation were obtained from the microbiological laboratories department, Faculty of Science, Cairo University after their isolation and identification.

2.6.1. Preparation of Inoculum

Briefly, each isolate was morphologically examined, and then colonies were selected from an agar plate culture and transferred into a nutrient broth medium and incubated at 37 °C for 24 h. Inoculum turbidity was compared with 0.5 McFarland standards containing 10⁸ CFU/mL.

2.6.2. Disc Diffusion Assay

Sabouraud dextrose agar (SDA) for yeast and fungal strains and Mueller-Hinton (MHA) for bacterial strains were poured into Petri dishes. Pour the second layer of agar cultures with 0.5 McFarland standard (1.0 × 10⁸ CFU/mL) on the previous dishes. Sterile discs loaded with 100 µL of TiO₂ NPs were placed on the surface of inoculated dishes, and incubated at 37 °C for 24 h. Distilled water was used as a negative control, penicillin (P10 mg) and oxytetracycline (OT30 mg) were kept as positive controls for bacterial and fungal strains. The results were determined by the mean zone of inhibition (MZI) and expressed in millimeters (mm) with a standard deviation for each microbial strain at the end of incubation periods. Each experiment was performed in triplicate.

2.6.3. Minimum Inhibitory Concentration (MIC) of TiO₂ Nanoparticles

MIC of TiO₂ NPs was carried out by using the broth dilution method (CLSI, M7-A7, 2006). Microbial strains were grown in nutrient broth at 37 °C overnight. Briefly, 100 µL of MHB, and 10 µL microbial suspension (1–2 × 10⁸ CFU/mL) were added to each tube. Finally, serial dilutions 20–40–60–80–100–120–140 µL/mL of TiO₂ NPs were added; negative control tube (containing MHB, and inoculum) and positive control (containing MHB, inoculum and penicillin (P10 mg) or oxytetracycline (OT30 mg)). The lowest concentra-

tion showing visual growth inhibition was considered as the MIC of TiO₂ NPs for the respective organism.

2.6.4. Minimum Bactericidal Concentration (MBC) of TiO₂ Nanoparticles

Briefly, 10 µL of suspension from each MIC dilution tube was inoculated on a nutrient agar plate and incubated at 37 °C for 24 h. The same was repeated for control tubes (positive and negative). No colonies on agar plates were formed due to the concentration of TiO₂ NPs which causes the bactericidal effect.

2.7. Cytotoxic Assay of TiO₂ Nanoparticles

2.7.1. Mammalian Cell Line

SKOV-3 cells (ovarian adenocarcinoma cell line) were obtained from the American Type Culture Collection (ATCC, Manassas, VA, USA). In Dulbecco's modified Eagle's medium (DMEM) enhanced with ten percent of heat-inactivated fetal bovine serum, one percent L-glutamine, buffer of HEPES, and 50 µg/mL gentamycin, the cells were cultured. At 37 °C in a humidified atmosphere with 5% CO₂, the cells were maintained and then subcultured two times a week [36].

2.7.2. Cytotoxicity Evaluation

The cytotoxicity of TiO₂ nanoparticles against SKOV-3 cells (ovarian adenocarcinoma cell line) was assayed by MTT colorimetric method [37]. The 50% inhibitory concentration (IC₅₀) is the concentration required to produce toxic effects in 50% of healthy cells.

2.8. Statistical Analysis

GraphPad Prism 5 was used for the statistical analysis of the results. One-way analysis of variance was used to analyze statistical significance of results, followed by Tukey's multiple comparison tests. Results are expressed as mean ± standard error (SE). Results were considered significant at $p < 0.05$.

3. Results

3.1. Chemical Constituents of *Juniperus phoenicea* Leaf Extract

GC/MS analysis of *Juniperus phoenicea* leaf extract revealed the identification of 24 compounds (Figure 1 and Table 1) belonging to different chemical categories. *Juniperus phoenicea* leaf extract consisted of 47.255% monoterpene hydrocarbons; β-Phellandrene (17.55%) was the major component in this fraction. The sesquiterpene hydrocarbons represented 26.865% consisting mainly of α-Humulene (20.95%). The oxygenated sesquiterpene and terpene represented 20.1% and 7.495% respectively. Other minors as alkane hydrocarbon, fatty acids, and Hydrocinnamic acid were present at 1.7%, 0.1%, and 0.12% respectively. The present study first time reports the chemical composition of aqueous extract from *J. phoenicea* leaves, analyzed by gas chromatography–mass spectrometry (GC-MS).

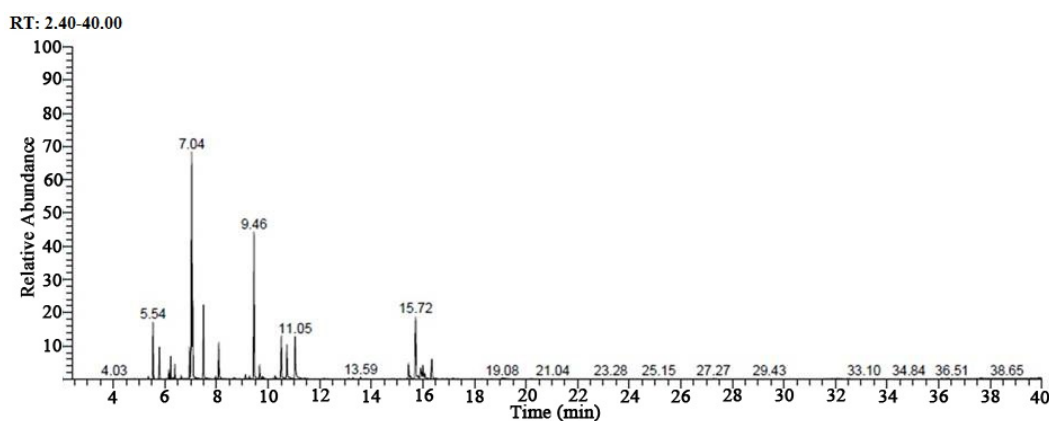


Figure 1. The GC/MS chromatogram of the analysis of *Juniperus phoenicea* leaf extract.

Table 1. GC/MS analysis of *Juniperus phoenicea* leaf extract.

Peak No.	Compound Name	RT	RC (%)	Probability
1	Sabinene	5.54	5.25	85.86
2	α -Humulene	7.04	20.95	71.80
3	β -Pinene	7.49	6.71	19.41 *
4	β -Myrcene	8.09	4.485	68.40
5	β -Phellandrene	9.46	17.55	36.60 *
6	α -Pinene	9.67	1.935	35.11 *
7	L-Limonene	10.51	6.09	30.64 *
8	α -Terpinolene	10.73	5.235	47.84
9	Linalool	11.05	7.335	51.35
10	β -Selinene	15.45	2.505	62.44
11	Elemol	15.72	7.62	52.05
12	Hexadecane	16.00	1.47	29.44 *
13	α -Cadinol	16.08	1.45	72.76
14	Isospathulenol	16.35	0.75	20.02 *
15	α -Amorphene	16.93	2.69	29.37 *
16	β -Citronellol	17.18	0.16	17.95 *
17	Cedrol	19.17	0.26	61.71
18	α -Muurolene	21.04	0.31	52.43
19	Cedreanol	25.15	0.2	26.73 *
20	δ -Cadinene	27.27	0.19	25.59 *
21	α -Cubebene	29.43	0.22	19.65 *
22	Nonacosane	33.10	0.23	25.32 *
23	Hexadecanoic acid	34.84	0.1	21.39 *
24	Benzenepropanoic acid	38.65	0.12	22.62 *

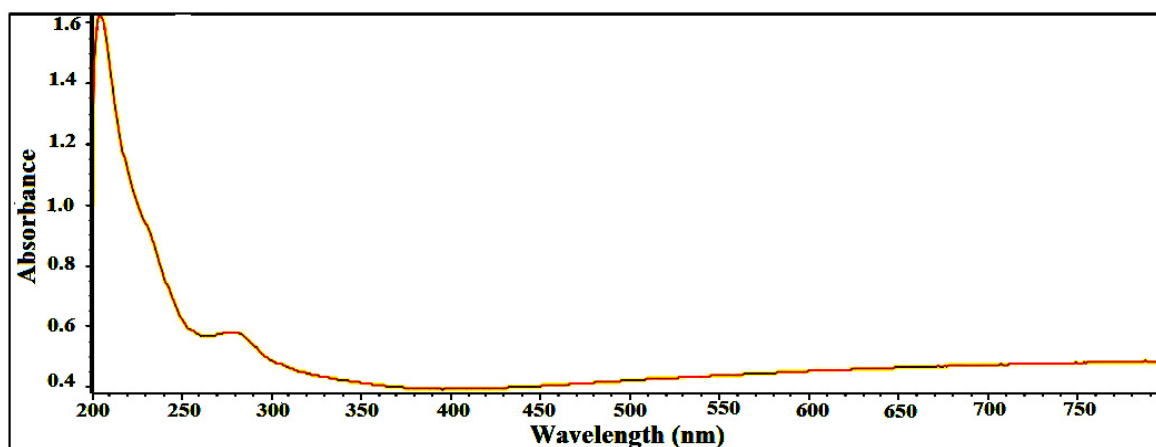
* indicates a tentative identification and probability % is less than 50%.

3.2. Synthesis and Characterization of TiO₂ Nanoparticles

Titanium dioxide nanoparticles were synthesized using leaf extract of *Juniperus phoenicea* and characterized using UV-Vis, DLS, TEM, XRD, and FT-IR spectroscopy.

3.2.1. UV-Vis spectroscopy of TiO₂ NPs

Figure 2 displays the UV-Vis absorption spectra of biosynthesized TiO₂ nanoparticles. A prominent peak at 205.4 nm with absorbance equal to 1.6 is seen. The strong peak at 205.4 nm in the range of 200 to 800 nm confirmed the biosynthesis of TiO₂ NPs using leaf extract of *Juniperus phoenicea*.

**Figure 2.** UV-Vis absorption spectra of TiO₂ NPs.

3.2.2. Dynamic Light Scattering (DLS)

DLS measurements were used to study the TiO₂ nanoparticles size distribution. Figure 3 shows a typical dynamic light scattering histogram of green synthesized titanium dioxide nanoparticle with the average particle size (hydrodynamic diameter) equal to (74.8 ± 0.649) nm.

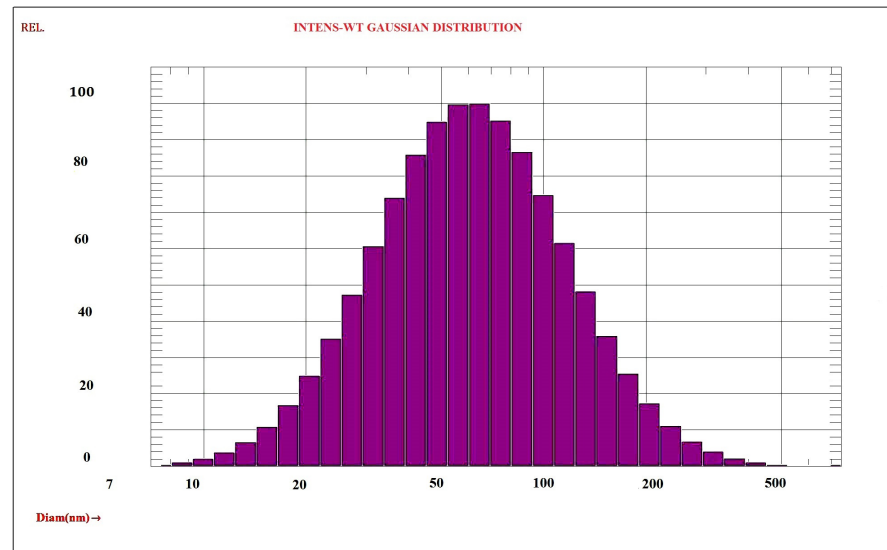


Figure 3. Dynamic light scattering histogram of green synthesized titanium dioxide nanoparticle.

3.2.3. Transmission Electron Microscopy (TEM)

TEM image of the biosynthesized TiO₂ NPs (Figure 4) revealed that the morphology of the biosynthesized titanium oxide nanoparticles possesses a uniform spherical structure in shape having a diameter in the range of 10–30 nm.

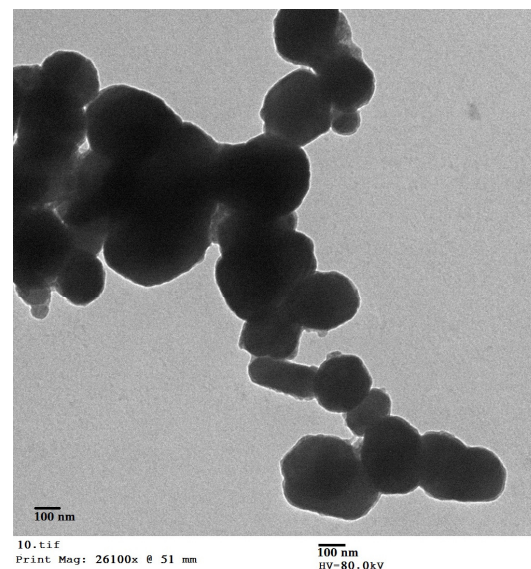


Figure 4. Transmission electron microscopy (TEM) image of the biosynthesized TiO₂ NPs.

3.2.4. X-ray Diffraction Spectroscopic Analysis (XRD)

Figure 5 represented XRD pattern of biosynthesized titanium oxide nanoparticles using *Juniperus phoenicea* leaf extract. Nine distinct peaks at $2\theta = 27.1^\circ, 35.7^\circ, 40.8^\circ, 43.9^\circ, 53.9^\circ, 56.0^\circ, 63.9^\circ, 68.8^\circ,$ and 69.8° that can be indexed as (110), (101), (111), (210), (211), (220), (310), (301), and (112) Miller indices. The JCPDS Card no. 21-1276. The existence of peak pattern confirmed the crystal structure of TiO₂ NPs. XRD pattern showed the crystalline

nature of the TiO₂ nanoparticles and the calculated average size of TiO₂ nanoparticles ~10 nm. The peaks sharpness and the absence of unknown peaks confirmed the crystalline nature and high purity of the biosynthesized TiO₂ NPs.

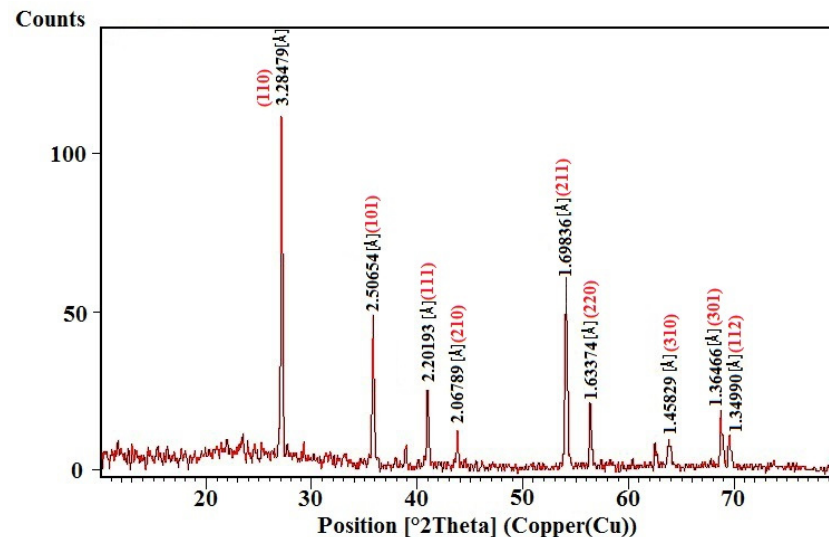


Figure 5. X-ray diffraction spectroscopic analysis (XRD) of the biosynthesized TiO₂ NPs.

3.2.5. Fourier Transform Infrared Spectroscopy (FTIR)

FTIR spectrum of biosynthesized titanium dioxide nanoparticles using *Juniperus phoenicea* leaf extract revealed peaks at 3851.01, 3449.51, 2084.14, 1636.36, 1045.34, and 553.48 cm⁻¹ (Figure 6). Peak observed at 3851, 3449 cm⁻¹ denote the O–H stretching of alcohols and phenolic compounds, and peaks at 2084.14, 1636.36 cm⁻¹ correspond to the C–O stretching, C=O stretching mode of the carbonyl functional groups in esters, ethers, acids and alcohol and C=C stretching (alkene). Peak at 1045 indicates the C–N stretching of aliphatic amines and the peak observed at 553 cm⁻¹ coincides with the Ti–O–Ti stretching vibration of TiO₂ NPs.

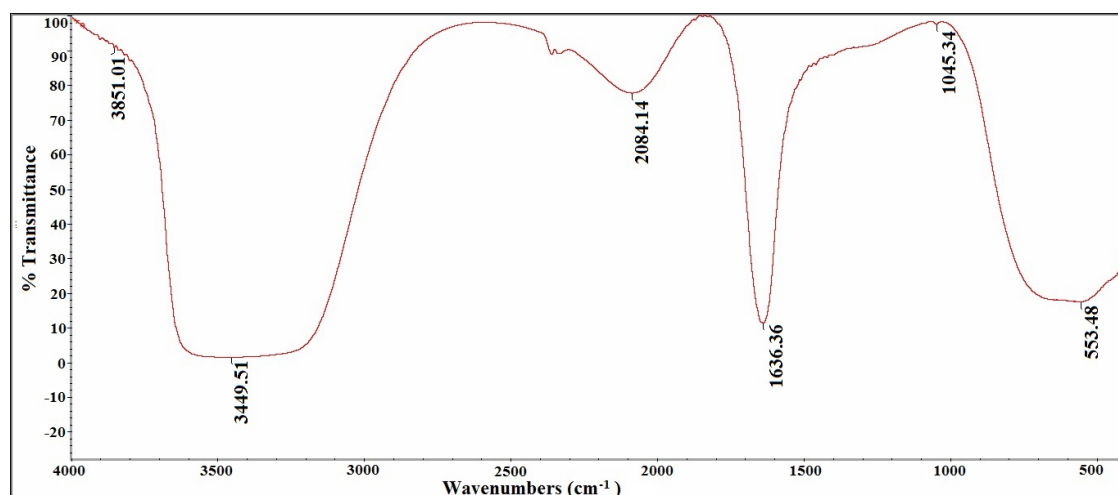


Figure 6. FTIR spectrum of the biosynthesized TiO₂ NPs.

3.3. Antimicrobial Efficacy of TiO₂ NPs

TiO₂ NPs synthesized using *Juniperus phoenicea* extract, showed efficacy against tested bacterial and fungal strains (Table 2). TiO₂ NPs caused growth inhibition for all tested microbial strains (Figure 7). Bacterial strains sensitive against TiO₂ NPs, but resistant to positive control were recorded, while fungal strains are more sensitive against TiO₂

NPs compared to positive control. Titanium dioxide nanoparticles showed maximum activity against *Asp. niger* with mean of zone inhibition (MZI) 30.3 ± 0.25 mm, followed by *Pen. digitatum*, *S. cerevisiae*, *B. subtilis* by MZI 25.2 ± 0.27 , 25.4 ± 0.36 , and 25.5 ± 0.31 at 100 $\mu\text{L/mL}$ respectively. TiO_2 NPs have a good performance against Gram positive bacteria (*B. subtilis* and *S. aureus*) compared to Gram negative bacteria (*K. pneumoniae* and *E. coli*). The biosynthesized nanoparticle showed a lowest MIC against *Asp. niger* and bactericidal MBC at ~ 20 and 40 $\mu\text{L/mL}$ respectively followed by other fungal strains and Gram positive bacteria. The highest degree scored of MIC and MBC by TiO_2 NPs against Gram negative bacteria ~ 80 and 140 $\mu\text{L/mL}$.

Table 2. Antimicrobial efficacy of TiO_2 NPs analyzed by disc diffusion technique, minimal inhibition concentration (MIC), and minimum bactericidal concentration (MBC).

Microbial Strains	Zone of Inhibition (mm, mean \pm SE)	MIC ($\mu\text{L/mL}$)	MBC ($\mu\text{L/mL}$)	* Oxytetracycline 30 mg	* Penicillin 10 mg
<i>S. aureus</i>	23.3 ± 0.27	40	80	ND	-
<i>B. subtilis</i>	25.5 ± 0.31	40	80	ND	-
<i>E. coli</i>	20.9 ± 0.28	80	120	ND	-
<i>K. pneumoniae</i>	15.7 ± 0.45	80	140	ND	-
<i>S. cerevisiae</i>	25.4 ± 0.36	40	80	-	15 ± 0.3
<i>Asp. niger</i>	30.3 ± 0.25	20	40	-	15 ± 0.2
<i>Pen. digitatum</i>	25.2 ± 0.27	40	100	-	17 ± 0.1

The values are presented as the mean of three replicates \pm the standard deviation. * (OT30) and (P10) were used as positive controls: ND; not detected.

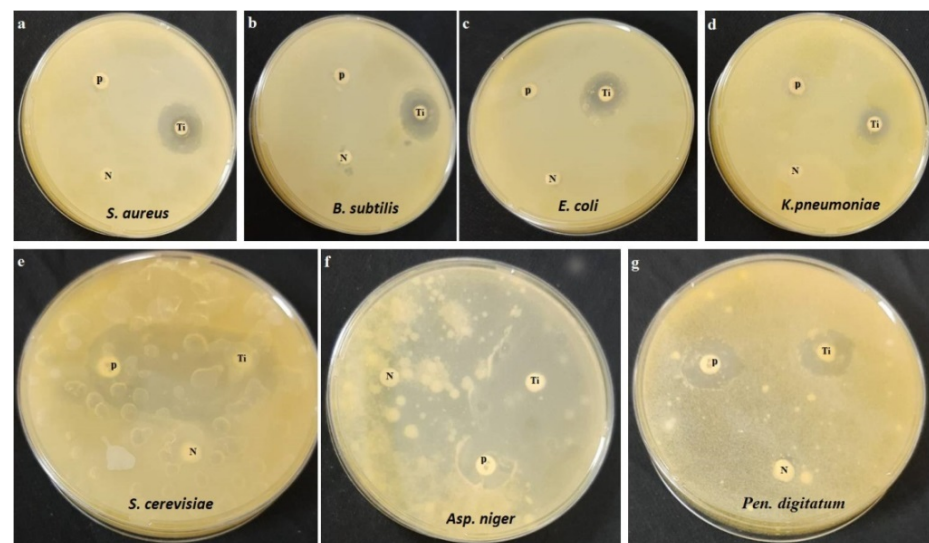


Figure 7. The antimicrobial efficacy of biosynthesized TiO_2 NPs against tested microbial strains. (a): *S. aureus*; (b): *B. subtilis*; (c): *E. coli*; (d): *K. pneumoniae*; (e): *S. cerevisiae*; (f): *Asp. Niger*; (g): *Pen. digitatum*. (P) positive control; (N) negative control; (Ti) TiO_2 NPs.

3.4. Cytotoxic Activity

Results revealed that synthesized TiO_2 nanoparticles showed significant inhibitory activity against human ovarian adenocarcinoma cells ($86.61 \pm 0.65\%$, $94.36 \pm 0.42\%$) at 250, 500 $\mu\text{g/mL}$ of TiO_2 nanoparticles, respectively with $\text{IC}_{50} = 50.13 \pm 1.65$ $\mu\text{g/mL}$. Figure 8 summarized the microscopic observation of the ovarian adenocarcinoma cell line (SKOV-3) treated with different concentrations of synthesized TiO_2 nanoparticles.

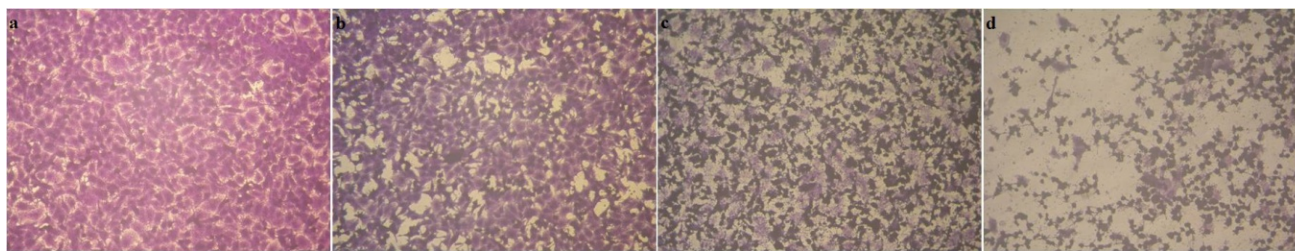


Figure 8. Morphological alterations of ovarian adenocarcinoma cell line (SKOV-3) treated with synthesized TiO_2 nanoparticles concentrations for 24 h (a): Control; (b): 20 $\mu\text{g/mL}$; (c): 100 $\mu\text{g/mL}$; (d): 500 $\mu\text{g/mL}$ 100 \times .

4. Discussion

The *Juniperus* Spp. is a group of traditionally utilized medicinal plants which are known to be involved in the prevention of various diseases. These plants are reported to contain several bioactive compound classes including glycosides, alkaloids, polyphenols, terpenoids, fatty acids and cinnamic acid derivatives [38,39]. Further, these bioactive compounds can be useful as reducing agents for the reaction with silver ions and as scaffolds directing the AgNP formation in solution [40,41]. In the present study, the synthesis of TiO_2 NPs was mainly analyzed by UV-Vis spectroscopy (200–800 nm) and other techniques of characterization [42]. A strong peak of absorbance occurred at 205.4 nm, in the range of 200 to 800 nm and confirmed the biosynthesis of TiO_2 NPs using leaf extract of *Juniperus phoenicea* confirming the formation of TiO_2 NPs [43]. The findings of TEM analysis are in line with the former works that reported that the small spherical-shaped TiO_2 NPs synthesized utilizing the leaf extract of the *Azadirachta indica* had a size range from 15 to 50 nm [44,45], or *Aloe vera* with an average size of 20 nm [17].

The graph of particle size distribution of TiO_2 NPs displayed average particle size (hydrodynamic diameter) of (74.8 ± 0.649) nm. Whereas, in a previous work, the leaf extract of *Juniperus procera* synthesized large-sized nanoparticles with a broad size distribution ranged from 30–90 nm [46].

All points in the XRD pattern can be determined well as tetragonal rutile phase of TiO_2 NPs and the diffraction data were in good agreement with JCPDS files no. 21-1276 [47]. The nature of plant sources and the quantity of plant extract and their photochemical constituents define the crystal structure and structural alignment of the prepared nanoparticles [48].

FT-IR spectrum of TiO_2 nanoparticles revealed very strong three peaks at 3449.51, 1636.36, and 553.48 cm^{-1} which were referred to -OH stretching vibration (indicating a large volume of O–H-stretched phenolic compounds), and bending vibration of O–Ti–O bond in *Juniperus phoenicea* leaves extract. This bonding may be attributed to the strong interaction (capped) of biomolecules with TiO_2 nanoparticles. Similar peaks (3433.85 cm^{-1} to 575.92 cm^{-1}) were reported and seen for TiO_2 NPs synthesized using the *Kniphofia foliosa* root extract [49]. The stabilizing effect of *Juniperus phoenicea* is not only due to having aromatic rings in hydrocinnamic acid but the presence of C=C bonds in monoterpene and sesquiterpene and carboxylic groups in hydrocinnamic acid.

The results confirmed the existence of phenolic compounds such as flavonoids, anthraquinones, and terpene existing in the *Juniperus phoenicea* leaf extract which plays an effective role in stabilizing/capping agent for TiO_2 nanoparticles formation as reported by [40,41,50]. Similar observations were also reported by [51,52].

The present results showed that TiO_2 nanoparticles synthesized using *Juniperus phoenicea* exhibited greater efficacy against fungal strains, *Asp. niger* followed by *Pen. digitatum*, and *S. cerevisiae* with mean of inhibition zone (MIZ) 30.3 ± 0.25 mm, 25.2 ± 0.27 , and 25.4 ± 0.36 respectively. A study by [53] showed moderate activity of synthesized Ag-NPs from *Juniperus procera* extract against *Pen. aeruginosa* (11.50 ± 0.29 mm) and *C. albicans* (14.30 ± 0.60 mm). Moreover, the present study showed that TiO_2 NPs have good effect

against *S. aureus* and *B. subtilis* as Gram positive followed by *E. coli* and *K. pneumoniae* as Gram negative, which is the same result as [18,53]. Whereas the result was better than previously reported studies [53–56]. Data of this paper's MIC and MBC of TiO₂ NPs correlate well with those of disc diffusion assay. The lowest MIC and MBC values; 40 µL/mL and 80 µL/mL of nanoparticles, were reported against *S. aureus* and *B. subtilis*. The present study's results are in line with [45], but against *Salmonella typhi*, *Escherichia coli*, and *K. pneumoniae*.

The presence of a high amount of terpenoids, flavonoids, and proteins in *Juniperus phoenicea* is responsible for the TiO₂ NPs formation and its stability as reported by [57–59] who showed that the different green materials used to stabilize and reduce metal ions are responsible for determining the colloidal stability and biological activities of the formed nanoparticles. However, antimicrobial potency of TiO₂ NPs is due to its uniform shape, size, and particle size distribution as well as colloidal stability of nanoparticles interacting with the microbial pathogens cell wall [60]. Green synthesis of TiO₂ nanoparticles using *Juniperus phoenicea* shows greater performance on microbial strains due to the interaction between microbial agents and metal ion surfaces [45,61]. Antibacterial effect of biosynthesized TiO₂ nanoparticles is due to the dissolving of the outer cell wall of bacteria, causing its death. TiO₂ nanoparticles are widespread in the outer cell wall of bacteria due to the presence of a hydroxyl group. The liberated ions may react with the cell wall of the bacteria, expediting the breakdown of the bacterial cell wall and showing antibacterial properties. In addition, TiO₂ nanoparticles cause the production of reactive oxygen species (ROS) inside the pathogens [62], and due to the accumulation of free radicals that readily interact with the pathogen's cell membrane, which in turn, results in pores, causing the death of the microbial pathogens [63,64].

The present results showed that the synthesized TiO₂ nanoparticles had a significant inhibitory activity against human ovarian adenocarcinoma cells with IC₅₀ = 50.13 ± 1.65 µg/mL. [65] revealed that TiO₂ NPs using aqueous *Coleus aromaticus* leaf extract had an amazing (92.37%) cytotoxic efficacy on the HeLa cell line at 100 µg/mL during 24 h of exposure. TiO₂ NPs synthesized using the orange peel extract had an inhibitory activity of 41% against A549 cell line at the concentration of 400 µg/mL [66]. The results are in accordance to the studies of [65,66]. The cytotoxicity of synthesized TiO₂ nanoparticles was probably due to the presence of capping elements of the plant extract on TiO₂ NPs, and the plant extract could provide excess electrons to the TiO₂ NPs, which might stimulate the accumulation of the reactive oxygen species (ROS) on the surface of the human ovarian adenocarcinoma cell line as reported by [67]. It leads to increased oxidative stress, cell membrane destruction, enhanced lipid peroxidation, reduced glutathione (GSH) level, and ultimately contributing to cell death [68].

The predominant compounds identified in the plant include β-phellandrene, α-humulene, linalool, elemol, and β-pinene. The present results on the same line of the previous study of Keskes et al., [69] reported that β-phellandrene, α-humulene, are the main compounds in hexane extract from *J. phoenicea* leaves. Further, compounds such as β-pinene, β-phellandrene, and L-limonene have a lower probability index compared to the other compounds. Hence, it can be represented as a tentative identification only and further studies in this line are necessary to have clear information. Supporting the observations, the presence of α-pinene and delta-3-carene were also reported by Ennajar, et al. [39]. These identified compounds are also known to be associated with various biological activities such as antioxidant and anti-inflammatory effects, antidiabetic effects, anticancer properties, and so on [57,70–73]. Previous studies by Al-Mustafa et al. [38] and Ennajar et al. [39] also observed similar constituents chemicals in the extract of *Juniperus phoenicea* leaves. It is also possible that the bioactive molecules observed in the leaf extract of *Juniperus phoenicea* act as capping and reducing agents due to their antioxidant potentials. It is therefore possible that the formation of white colored TiO₂ NPs might be due to the reducing reaction of these bioactive compounds.

5. Conclusions

In conclusion, the study successfully synthesized titanium dioxide nanoparticles using *Juniperus phoenicea* leaf extract. Their constituents were identified by GC-MS analysis and the data revealed that some components such as elemol, linalool, and hydrocinnamic acid in *Juniperus phoenicea* plant due to having hydroxyl functional groups act as reducing agents. Moreover, carboxyl groups and benzyl rings in other components act as stabilizing agents. The characterization of eco-friendly synthesized titanium dioxide nanoparticles were confirmed by UV-Vis, DLS, TEM, FT-IR spectroscopy, and XRD analyses. Biosynthesized titanium dioxide nanoparticles showed antibacterial and antifungal properties against some bacterial and fungal strains. Moreover, it showed cytotoxic activity on the human ovarian adenocarcinoma cells. Furthermore, it was concluded that biosynthesized titanium dioxide nanoparticles can be used in medicine as curative agents according to its in vitro antibacterial, antifungal, and cytotoxic activities. TiO₂ nanoparticles using *Juniperus phoenicea* leaf extract could be applied for the wastewater handling and pollutants degradation.

Author Contributions: Conceptualization, L.M.A.M. and H.H.; methodology, H.H., L.M.A.M., A.S.A. and A.A.Z.; validation, L.M.A.M., A.S.A., H.H. and A.A.Z.; formal analysis, H.H. and A.A.Z.; investigation, H.H., L.M.A.M., A.A.Z. and A.S.A.; resources, H.H. and L.M.A.M.; data curation, A.A.Z. and A.S.A.; writing—original draft preparation, H.H., L.M.A.M., A.A.Z. and A.S.A.; writing—review and editing, H.H. and A.A.Z. project administration, L.M.A.M. and A.S.A.; funding acquisition, L.M.A.M. All authors have read and agreed to the published version of the manuscript.

Funding: This research was funded by Taif University a support project (1/443/6), Taif University, Taif, Saudi Arabia.

Institutional Review Board Statement: Not applicable.

Informed Consent Statement: Not applicable.

Data Availability Statement: Not applicable.

Acknowledgments: Authors are thankful to the Deanship of Scientific Research at Taif University for funding this work (1/443/6), Taif University, Taif, Saudi Arabia.

Conflicts of Interest: The authors declare no conflict of interest.

Sample Availability: Samples of the compounds are available from the authors.

References

1. Ciesla, W.M. *Non-Wood Forest Products from Conifers*; Food and Agriculture Organization of the United Nations (FAO): Rome, Italy, 1998.
2. Tilford, G.L. *Edible and Medicinal Plants of the West*; Mountain Press Publishing Company: Missoula, Montana, 1997.
3. Manniche, L. *Sacred Luxuries: Fragrance, Aromatherapy, and Cosmetics in Ancient Egypt*; Cornell University Press: New York, NY, USA, 1999; p. 21.
4. Bolous, L. *Flora of Egypt*; Al Hadara Publishing: Cairo, Egypt, 1999.
5. El-Sawi, S.A.; Motawae, H.M.; Sleem, M.A.; El-Shabrawy, A.O.; Sleem, A.; Ismail, M.A. Phytochemical screening, investigation of carbohydrate contents, and antiviral activity of *Juniperus phoenicea* L. growing in Egypt. *J. Herbs Spices Med. Plants* **2014**, *20*, 83–91. [\[CrossRef\]](#)
6. Aljaiyash, A.A.; Gonaïd, M.H.G.; Islam, M.; Chaouch, A. Antibacterial and cytotoxic activities of some Libyan medicinal plants. *J. Nat. Prod. Plant Resour.* **2014**, *4*, 43–51.
7. Tavares, L.; Carrilho, D.; Tyagi, M.; Barata, D.; Serra, A.T.; Duarte, C.M.M.; Duarte, R.O.; Feliciano, R.P.; Bronze, M.R.; Chicau, P.; et al. Neuroprotective effect of blackberry (*Rubus* sp.) polyphenols is potentiated after simulated gastrointestinal digestion. *Food Chem.* **2012**, *131*, 1443–1452. [\[CrossRef\]](#)
8. Eissa, T.A.; Palomino, O.M.; Carretero, M.E.; Gómez-Serranillos, M.P. Ethnopharmacological study of medicinal plants used in the treatment of CNS disorders in Sinai Peninsula, Egypt. *J. Ethnopharmacol.* **2014**, *151*, 317–332. [\[CrossRef\]](#)
9. Amer, M.M.A.; Wasif, M.M.; Abo-Aytta, A.M. Chemical and biological evaluation of *Juniperus phoenicea* as a hypoglycaemic agent. *J. Agric. Res.* **1994**, *21*, 1077–1091.
10. Pardos, J.A.; Pardos, M. *Enzyklopädie der Holzgewächse: Handbuch und Atlas der Dendrologie*; Roloff, A., Weisgerber, H., Lang, U.M., Stimm, B., Schütt, P., Eds.; Wiley-Vch Verlag: Weinheim, Germany, 2000; p. 3.
11. Farjon, A. *The IUCN Red List of Threatened Species*; The International Union for Conservation of Nature (IUCN): Gland, Switzerland, 2013; p. 42244/0+.

12. Öztürk, M.; Tümen, I.; Uğur, A.; Aydoğmus-Öztürk, F.; Topçu, G. Evaluation of fruit extracts of six Turkish *Juniperus* species for their antioxidant, anticholinesterase and antimicrobial activities. *J. Sci. Food Agric.* **2011**, *91*, 867–876. [\[CrossRef\]](#)
13. Šarić-Kundalić, B.; Dobeš, C.; Klatte-Asselmeyer, V.; Saukel, J. Ethnobotanical survey of traditionally used plants in human therapy of east, north and northeast Bosnia and Herzegovina. *J. Ethnopharmacol.* **2011**, *133*, 1051–1076. [\[CrossRef\]](#)
14. Ponarulselvam, S.; Panneerselvam, C.; Murugan, K.; Aarthi, N.; Kalimuthu, K.; Thangamani, S. Synthesis of silver nanoparticles using leaves of *Catharanthus roseus* Linn. G. Don and their ant plasmodial activities. *Asian Pac. J. Trop. Biomed.* **2012**, *2*, 574–580. [\[CrossRef\]](#)
15. Rajasekharreddy, P.; Rani, P.U. Biofabrication of Ag nanoparticles using *Sterculia foetida* L. seed extract and their toxic potential against mosquito vectors and HeLa cancer cells. *Mater. Sci. Eng. C Mater. Biol. Appl.* **2014**, *39*, 203–212. [\[CrossRef\]](#)
16. Verma, A.; Mehata, M.S. Controllable synthesis of silver nanoparticles using neem leaves and their antimicrobial activity. *J. Radiat. Res. Appl. Sci.* **2016**, *9*, 109–115. [\[CrossRef\]](#)
17. Rajkumari, J.; Magdalane, C.M.; Siddhardha, B.; Madhavan, J.; Ramalingam, G.; Al-Dhabi, N.A.; Arasu, M.V.; Ghilan, A.; Duraipandiayan, V.; Kaviyarasu, K. Synthesis of titanium oxide nanoparticles using Aloe barbadensis mill and evaluation of its antibiofilm potential against *Pseudomonas aeruginosa* PAO1. *J. Photochem. Photobiol. B.* **2019**, *201*, 111667. [\[CrossRef\]](#)
18. Maham, M.; Nasrollahzadeh, M.; Bagherzadeh, M.; Akbari, R. Green synthesis of palladium/titanium dioxide nanoparticles and their application for the reduction of methyl orange, congo red and rhodamine B in aqueous medium. *Comb Chem High Throughput Screen.* **2017**, *20*, 787–795. [\[CrossRef\]](#)
19. Nasrollahzadeh, M.; Atarod, M.; Jaleh, B.; Gandomirouzbahani, M. In situ green synthesis of Ag nanoparticles on graphene oxide/TiO₂ nanocomposite and their catalytic activity for the reduction of 4-nitrophenol, congo red and methylene blue. *Ceram. Int.* **2016**, *42*, 8587–8596. [\[CrossRef\]](#)
20. Rostami-Vartooni, A.; Nasrollahzadeh, M.; Salavati-Niasari, M.; Atarod, M. Photocatalytic degradation of azo dyes by titanium dioxide supported silver nanoparticles prepared by a green method using *Carpobrotus acinaciformis* extract. *J. Alloys Compd.* **2016**, *689*, 15–20. [\[CrossRef\]](#)
21. Saxena, A.; Tripathi, R.M.; Zafar, F.; Singh, P. Green synthesis of silver nanoparticles using aqueous solution of *Ficus benghalensis* leaf extract and characterization of their antibacterial activity. *Mater. Lett.* **2012**, *67*, 91–94. [\[CrossRef\]](#)
22. Dubey, S.B.; Lahtinen, M.; Sillanpää, M. Green synthesis and characterizations of silver and gold nanoparticles using leaf extract of *Rosa rugosa*. *Colloids Surf. A Physicochem. Eng. Asp.* **2010**, *364*, 34–41. [\[CrossRef\]](#)
23. Rai, R.V.; Bai, J.A. *Nanoparticles and Their Potential Application as Antimicrobials*, *Science against Microbial Pathogens: Communicating Current Research and Technological Advances*; Méndez-Vilas, A., Ed.; Microbiology Series, No. 3, 1; Formatex: Badajoz, Spain, 2011; pp. 197–209.
24. Luo, P.G.; Tzeng, T.R.; Shah, R.R.; Stutzenberger, F.J. Nanomaterials for antimicrobial applications and pathogen detection. *Curr. Trends Microbiol.* **2007**, *3*, 111–128.
25. Amarnath, C.A.; Nanda, S.S.; Papaefthymiou, G.C.; Yi, D.K.; Paik, U. Nanohybridization of low-dimensional nanomaterials: Synthesis, classification and application. *Crit. Rev. Solid State Mater. Sci.* **2013**, *38*, 1–56. [\[CrossRef\]](#)
26. Anjum, S.; Ishaque, S.; Fatima, H.; Farooq, W.; Hano, C.; Abbasi, B.H.; Anjum, I. Emerging Applications of Nanotechnology in Healthcare Systems: Grand Challenges and Perspectives. *Pharmaceuticals* **2021**, *14*, 707. [\[CrossRef\]](#)
27. Anjum, S.; Hashim, M.; Malik, S.A.; Khan, M.; Lorenzo, J.M.; Abbasi, B.H.; Hano, C. Recent Advances in Zinc Oxide Nanoparticles (ZnO NPs) for Cancer Diagnosis, Target Drug Delivery, and Treatment. *Cancers* **2021**, *13*, 4570. [\[CrossRef\]](#)
28. Anjum, S.; Khan, A.K.; Qamar, A.; Fatima, N.; Drouet, S.; Renouard, S.; Blondeau, J.P.; Abbasi, B.H.; Hano, C. Light Tailoring: Impact of UV-C Irradiation on Biosynthesis, Physiognomies, and Clinical Activities of *Morus macroura*-Mediated Monometallic (Ag and ZnO) and Bimetallic (Ag–ZnO) Nanoparticles. *Int. J. Mol. Sci.* **2021**, *22*, 11294. [\[CrossRef\]](#)
29. Khan, A.K.; Renouard, S.; Drouet, S.; Blondeau, J.-P.; Anjum, I.; Hano, C.; Abbasi, B.H.; Anjum, S. Effect of UV Irradiation (A and C) on *Casuarina equisetifolia*-Mediated Biosynthesis and Characterization of Antimicrobial and Anticancer Activity of Biocompatible Zinc Oxide Nanoparticles. *Pharmaceutics* **2021**, *13*, 1977. [\[CrossRef\]](#)
30. Alam, H.; Khatoon, N.; Raza, M.; Prahlad Ghosh, C.; Sardar, M. Synthesis and Characterization of Nano Selenium Using Plant Biomolecules and Their Potential Applications. *BioNanoSci.* **2019**, *9*, 96–104. [\[CrossRef\]](#)
31. Davies, N.W. Gas chromatographic retention indices of monoterpenes on methyl silicone and Carbowax 20M phases. *J. Chromatogr.* **1990**, *503*, 1–24. [\[CrossRef\]](#)
32. Javed, B.; Raja, N.I.; Nadhman, A.; Mashwani, Z.-R. Understanding the potential of bio-fabricated non-oxidative silver nanoparticles to eradicate *Leishmania* and plant bacterial pathogens. *Appl. Nanosci.* **2020**, *10*, 2057–2067. [\[CrossRef\]](#)
33. Mangadlao, J.D.; Wang, X.; McCleese, C.; Escamilla, M.; Ramamurthy, G.; Wang, Z.; Govande, M.; Basilion, J.P.; Burda, C. Prostate-Specific Membrane Antigen Targeted Gold Nanoparticles for Theranostics of Prostate Cancer. *ACS Nano* **2018**, *12*, 3714–3725. [\[CrossRef\]](#)
34. Zhang, H.; Chen, G. Potent antibacterial activities of Ag/TiO₂ nanocomposite powders synthesized by a one-pot sol-gel method. *Environ. Sci. Technol.* **2009**, *15*, 2905–2910. [\[CrossRef\]](#)
35. National Committee for Clinical Laboratory Standards. *Performance Standards for Antimicrobial Disk Susceptibility Tests*; Approved standard; NCCLS document M2-A5; National Committee for Clinical Laboratory Standards: Wayne, PA, USA, 1993.
36. Vijayan, P.; Raghu, C.; Ashok, G.; Dhanaraj, S.A.; Suresh, B. Antiviral activity of medicinal plants of Nilgiris. *Indian J. Med. Res.* **2004**, *120*, 24–29.

37. Mosmann, T. Rapid colorimetric assay for cellular growth and survival: Application to proliferation and cytotoxicity assays. *J. Immunol. Methods* **1983**, *65*, 55–63. [\[CrossRef\]](#)
38. Al-Mustafa, A.; Al-Tawarah, M.; Al-Sheraideh, M.S.; Al-Zahrany, F.A. Phytochemical analysis, antioxidant and in vitro β -galactosidase inhibition activities of *Juniperus phoenicea* and *Calicotome villosa* methanolic extracts. *BMC Chem.* **2021**, *15*, 55. [\[CrossRef\]](#)
39. Ennajar, M.; Bouajila, J.; Lebrhi, A.; Mathieu, F.; Abderraba, M.; Raies, A.; Romdhane, M. Chemical composition and antimicrobial and antioxidant activities of essential oils and various extracts of *Juniperus phoenicea* L. (Cupressaceae). *J. Food Sci.* **2009**, *74*, M364–M371. [\[CrossRef\]](#)
40. Al-Attar, A.M. Hepatoprotective influence of vitamin C on thioacetamide—induced liver cirrhosis in Wistar male rats. *J. Pharmacol. Toxicol.* **2011**, *6*, 218–288. [\[CrossRef\]](#)
41. Lai, J.-P.; Lim, Y.H.; Su, J.; Shen, H.-M.; Ong, C.N. Identification and characterization of major flavonoids and caffeoylquinic acids in three Compositae plants by LC/DAD-APCI/MS. *J. Chromatogr. B* **2007**, *848*, 215–225. [\[CrossRef\]](#)
42. Mehrizi, M.K.; Shahi, Z. *Application of Plant-Based Natural Product to Synthesize Nanomaterial*; Srivastava, M., Srivastava, N., Mishra, P., Gupta, V., Eds.; Nanomaterials in Biofuels Research. Clean Energy Production Technologies; Springer: Singapore, 2020; pp. 53–73.
43. Vijayalakshmi, R.; Rajendran, V. Synthesis and characterization of nano-TiO₂ via different methods. *Arch. Appl. Sci. Res.* **2012**, *4*, 1183–1190.
44. Anbalagan, K.; Mohanraj, S.; Pugalenti, V. Rapid phytosynthesis of nano-sized titanium using leaf extract of *Azadirachta indica*. *Int. J. Chem. Tech. Res.* **2015**, *8*, 2047–2052.
45. Thakur, B.K.; Kumar, A.; Kumar, D. Green synthesis of titanium dioxide nanoparticles using *Azadirachta indica* leaf extract and evaluation of their antibacterial activity. *S. Afr. J. Bot.* **2019**, *124*, 223–227. [\[CrossRef\]](#)
46. Ibrahim, E.; Kilany, M.; Ghramh, H.A.; Khan, K.; Islam, S.U. Cellular proliferation/cytotoxicity and antimicrobial potentials of green synthesized silver nanoparticles (AgNPs) using *Juniperus procera*. *Saudi J. Biol. Sci.* **2019**, *26*, 1689–1694. [\[CrossRef\]](#)
47. Lin, J.; Heo, Y.U.; Nattestad, A.; Sun, Z.; Wang, L.; Kim, J.H.; Dou, S.X. 3D hierarchical rutile TiO₂ and metal-free organic sensitizer producing dye-sensitized solar cells 8.6% conversion efficiency. *Sci. Rep.* **2014**, *4*, 5769. [\[CrossRef\]](#)
48. Kuchekar, S.R.; Patil, M.P.; Gaikwad, V.B.; Han, S.-H. Synthesis and characterization of silver nanoparticles using *Azadirachta indica* (Neem) leaf extract. *Int. J. Eng. Sci. Invent.* **2017**, *6*, 66–70.
49. Bekele, E.T.; Gonfa, B.A.; Zelekew, O.A.; Belay, H.H.; Sabir, F.K. Synthesis of Titanium Oxide Nanoparticles Using Root Extract of *Kniphofia foliosa* as a Template, Characterization, and Its Application on Drug Resistance Bacteria. *J. Nanomater.* **2020**, *2020*, 2817037. [\[CrossRef\]](#)
50. Ravikumar, P.; Kumar, S.S. Antifungal activity of extracellularly synthesized silver nanoparticles from *Morinda citrifolia* L. *Int. J. Tech. Res. Appl.* **2014**, *2*, 108–111.
51. Vasconcelos, D.C.; Costa, V.C.; Nunes, E.H.; Sabioni, A.C.; Gasparon, M.; Vasconcelos, W.L. Infrared spectroscopy of titania sol-gel coatings on 316L stainless steel. *Mater. Sci. Appl.* **2011**, *2*, 1375–1382. [\[CrossRef\]](#)
52. Yilmaz, M.; Turkdemir, H.; Kilic, M.A.; Bayram, E.; Cicek, A.; Mete, A.; Ulug, B. Biosynthesis of silver nanoparticles using leaves of *Stevia rebaudiana*. *Mater. Chem. Phys.* **2011**, *130*, 1195–1202. [\[CrossRef\]](#)
53. Khan, M.; Karupiah, P.; Alkhatlan, H.Z.; Kuniyil, M.; Khan, M.; Adil, S.F.; Shaik, M.R. Green Synthesis of Silver Nanoparticles Using *Juniperus procera* Extract: Their Characterization, and Biological Activity. *Crystals* **2022**, *12*, 420. [\[CrossRef\]](#)
54. Ansari, A.; Siddiqui, V.U.; Rehman, W.U.; Akram, M.K.; Siddiqi, W.A.; Alosaimi, A.M.; Hussein, M.A.; Rafatullah, M. Green Synthesis of TiO₂ Nanoparticles Using *Acorus calamus* Leaf Extract and Evaluating Its Photocatalytic and In Vitro Antimicrobial Activity. *Catalysts* **2022**, *12*, 181. [\[CrossRef\]](#)
55. Chawla, V.; Sathaye, S. Biosynthesis of silver nanoparticles using methanolic extracts of *Acorus calamus*, and assessment of its antioxidant and antimicrobial activity. *J. Med. Plants Stud.* **2017**, *5*, 358–363.
56. Ganesan, R.; Gurumallesu Prabu, H. Synthesis of gold nanoparticles using herbal *Acorus calamus* rhizome extract and coating on cotton fabric for antibacterial and UV blocking applications. *Arab. J. Chem.* **2019**, *12*, 2166–2174. [\[CrossRef\]](#)
57. Rónavári, A.; Kovács, D.; Igaz, N.; Vágvolgyi, C.; Boros, I.M.; Kónya, Z.; Pfeiffer, I.; Kiricsi, M. Biological activity of green-synthesized silver nanoparticles depends on the applied natural extracts: A comprehensive study. *Int. J. Nanomed.* **2017**, *12*, 871–883. [\[CrossRef\]](#) [\[PubMed\]](#)
58. Rónavári, A.; Igaz, N.; Gopisetty, M.K.; Szerencsés, B.; Kovács, D.; Papp, C.G.; Vágvolgyi, C.; Boros, I.M.; Kónya, Z.; Kiricsi, M.; et al. Biosynthesized silver and gold nanoparticles are potent antimycotics against opportunistic pathogenic yeasts and dermatophytes. *Int. J. Nanomed.* **2018**, *13*, 695–703. [\[CrossRef\]](#)
59. Rónavári, A.; Béteky, P.; Boka, E.; Zakupszky, D.; Igaz, N.; Szerencsés, B.; Pfeiffer, I.; Kónya, Z.; Kiricsi, M. Polyvinyl-Pyrrolidone-Coated Silver Nanoparticles-The Colloidal, Chemical, and Biological Consequences of Steric Stabilization under Biorelevant Conditions. *Int. J. Mol. Sci.* **2021**, *22*, 8673. [\[CrossRef\]](#)
60. Chudasama, B.; Vala, A.K.; Andhariya, N.; Mehta, R.V.; Upadhyay, R.V. Highly bacterial resistant silver nanoparticles: Synthesis and antibacterial activities. *J. Nanoparticle Res.* **2010**, *12*, 1677–1685. [\[CrossRef\]](#)
61. Azizi-Lalabadi, M.; Ehsani, A.; Divband, B.; Alizadeh-Sani, M. Antimicrobial activity of Titanium dioxide and Zinc oxide nanoparticles supported in 4A zeolite and evaluation the morphological characteristic. *Sci. Rep.* **2019**, *9*, 17439. [\[CrossRef\]](#) [\[PubMed\]](#)

62. Morones, J.R.; Elechiguerra, J.L.; Camacho, A.; Holt, K.; Kouri, J.B.; Ramírez, J.T.; Yacaman, M.J. The bactericidal effect of silver nanoparticles. *Nanotechnology* **2005**, *16*, 2346–2353. [[CrossRef](#)]
63. Danilczuk, M.; Lund, A.; Sadlo, J.; Yamada, H.; Michalik, J. Conduction electron spin resonance of small silver particles. *Spectrochim. Acta Part A Mol. Biomol. Spectrosc.* **2006**, *63*, 189–191. [[CrossRef](#)]
64. Kim, J.S.; Kuk, E.; Yu, K.N.; Kim, J.-H.; Park, S.J.; Lee, H.J.; Kim, S.H.; Park, Y.K.; Park, Y.H.; Hwang, C.-Y.; et al. Antimicrobial effects of silver nanoparticles. *Nanomed. Nanotechnol. Biol. Med.* **2007**, *3*, 95–101, Erratum in *Nanomed. Nanotechnol. Biol. Med.* **2014**, *10*, e1119. [[CrossRef](#)] [[PubMed](#)]
65. Narayanan, M.; Vigneshwari, P.; Natarajan, D.; Kandasamy, S.; Alsehlhi, M.; Elfasakhany, A.; Pugazhendhi, A. Synthesis and characterization of TiO₂ NPs by aqueous leaf extract of *Coleus aromaticus* and assess their antibacterial, larvicidal, and anticancer potential. *Environ. Res.* **2021**, *200*, 111335. [[CrossRef](#)]
66. Amanulla, A.M.; Sundaram, R. Green synthesis of TiO₂ nanoparticles using orange peel extract for antibacterial, cytotoxicity and humidity sensor applications. *Mater. Today Proc.* **2019**, *8*, 323–331.
67. Lu, P.J.; Fang, S.W.; Cheng, W.L.; Huang, S.C.; Huang, M.C.; Cheng, H.F. Characterization of titanium dioxide and zinc oxide nanoparticles in sunscreen powder by comparing different measurement methods. *J. Food Drug Anal.* **2018**, *26*, 1192–1200. [[CrossRef](#)]
68. Mahmoudi, M.; Azadmanesh, K.; Shokrgozar, M.A.; Journeay, W.S.; Laurent, S. Effect of nanoparticles on the cell life cycle. *Chem. Rev.* **2011**, *111*, 3407–3432. [[CrossRef](#)]
69. Keskes, H.; Belhadj, S.; Jlaïl, L.; El Feki, A.; Damak, M.; Sayadi, S.; Allouche, N. LC-MS-MS and GC-MS analyses of biologically active extracts and fractions from Tunisian *Juniperus phoenicea* leaves. *Pharm. Biol.* **2017**, *55*, 88–95. [[CrossRef](#)]
70. Sneha, K.; Narayanankutty, A.; Job, J.T.; Olatunji, O.J.; Alfarhan, A.; Famurewa, A.C.; Ramesh, V. Antimicrobial and Larvicidal Activities of Different *Ocimum* Essential Oils Extracted by Ultrasound-Assisted Hydrodistillation. *Molecules* **2022**, *27*, 1456. [[CrossRef](#)]
71. Anusmitha, K.M.; Aruna, M.; Job, J.T.; Narayanankutty, A.; Benil, P.B.; Rajagopal, R.; Alfarhan, A.; Barcelo, D. Phytochemical analysis, antioxidant, anti-inflammatory, anti-genotoxic, and anticancer activities of different *Ocimum* plant extracts prepared by ultrasound-assisted method. *Phys. Mol. Plant Pathol.* **2022**, *117*, 101746. [[CrossRef](#)]
72. Sharma, M.; Grewal, K.; Jandrotia, R.; Batish, D.R.; Singh, H.P.; Kohli, R.K. Essential oils as anticancer agents: Potential role in malignancies, drug delivery mechanisms, and immune system enhancement. *Biomed. Pharmacother.* **2022**, *146*, 112514. [[CrossRef](#)] [[PubMed](#)]
73. Cascaes, M.M.; De Moraes, Â.A.B.; Cruz, J.N.; Franco, C.d.J.P.; Silva, R.C.E.; Nascimento, L.D.d.; Ferreira, O.O.; Anjos, T.O.d.; de Oliveira, M.S.; Guilhon, G.M.S.P.; et al. Phytochemical Profile, Antioxidant Potential and Toxicity Evaluation of the Essential Oils from *Duguetia* and *Xylopia* Species (Annonaceae) from the Brazilian Amazon. *Antioxidants* **2022**, *11*, 1709. [[CrossRef](#)] [[PubMed](#)]

Disclaimer/Publisher's Note: The statements, opinions and data contained in all publications are solely those of the individual author(s) and contributor(s) and not of MDPI and/or the editor(s). MDPI and/or the editor(s) disclaim responsibility for any injury to people or property resulting from any ideas, methods, instructions or products referred to in the content.